PASSAGE OF PARTICLES THROUGH MATTER

To reduce the size of this section's PostScript file, we have divided it into three PostScript files. We present the following index:

PART 1

Page #	Section name	
1	23.1	Notation
2	23.2	Ionization energy loss by heavy particles
7	23.3	Restricted energy loss rates for relativistic ionizing particles

PART 2

Page #	Section name	
8	23.4	Energetic knock-on electrons (δ rays)
8	23.5	Ionization yields
8	23.6	Multiple scattering through small angles
10	23.7	Radiation length and associated quantities
13	23.8	Electromagnetic cascades

PART 2

Page #	Section name	
17	23.9	Muon energy loss at high energy
19	23.10	Čerenkov and transition radiation
21		References

23. PASSAGE OF PARTICLES THROUGH MATTER

Revised May 1996 by D.E. Groom (LBNL).

23.1. Notation

Table 23.1: Summary of variables used in this section. The kinematic variables β and γ have their usual meanings.

Symbol	Definition	Units or Value
α	Fine structure constant	$1/137.035\,989\,5(61)$
M	Incident particle mass	MeV/c^2
E	Incident particle energy γMc^2	MeV
T	Kinetic energy	MeV
m_ec^2	Electron mass $\times$ c^2	$0.510\,999\,06(15)$ MeV
r_e	Classical electron radius $e^2/4\pi\epsilon_0 m_e c^2$	$2.817\,940\,92(38)$ fm
N_A	Avogadro's number	$6.022\,136\,7(36) \times 10^{23}$ mol^{-1}
ze	Charge of incident particle	
Z	Atomic number of medium	
A	Atomic mass of medium	g mol^{-1}
K/A	$4\pi N_A r_e^2 m_e c^2/A$	$0.307\,075$ MeV g^{-1} cm^2 for $A = 1$ g mol^{-1}
I	Mean excitation energy	eV
δ	Density effect correction to ionization energy loss	
$\hbar\omega_p$	Plasma energy $\sqrt{4\pi N_e r_e^3}\ m_e c^2/\alpha$	$28.816\sqrt{\rho\langle Z/A\rangle}$ eV$^{(a)}$
N_c	Electron density	(units of r_e)$^{-3}$
w_j	Weight fraction of the jth element in a compound or mixture	
n_j	$\propto$ number of jth kind of atoms in a compound or mixture	
X_0	Radiation length	g cm^{-2}
—	$4\alpha r e^2 N_A/A$	$(716.408$ g cm$^{-2})^{-1}$ for $A = 1$ g mol^{-1}
E_c	Critical energy	MeV
E_s	Scale energy $\sqrt{4\pi/\alpha}\ m_e c^2$	21.2052 MeV
R_M	Molière radius	MeV g^{-1} cm^2

$^{(a)}$ For ρ in g cm^{-3}.

23.2. Ionization energy loss by heavy particles [1–5]

Moderately relativistic charged particles other than electrons lose energy in matter primarily by ionization. If the incident particle velocity βc is larger than that of orbital electrons ($\sim Z\alpha c$) and small enough that radiative effects do not dominate (for example, pion energy smaller than 100–200 GeV in iron), then the mean rate of energy loss (or stopping power) is given by the Bethe-Bloch equation,

$$-\frac{dE}{dx} = Kz^2 \frac{Z}{A} \frac{1}{\beta^2} \left[\frac{1}{2} \ln \frac{2m_e c^2 \beta^2 \gamma^2 T_{\rm max}}{I^2} - \beta^2 - \frac{\delta}{2} \right] \ . \tag{23.1}$$

Here $T_{\rm max}$ is the maximum kinetic energy which can be imparted to a free electron in a single collision, and the other variables are defined in Table 23.1. The units are chosen so that dx is measured in mass per unit area, *e.g.*, in g cm^{-2}. The function as computed for pions on copper is shown by the solid curve in Fig. 23.1, and for pions on other materials in Fig. 23.2. A minor dependence on M at the highest energies is introduced through $T_{\rm max}$, but for all practical purposes in high-energy physics dE/dx in a given material is a function only of β. Except in hydrogen, particles of the same velocity have very similar rates of energy loss in different materials; there is a slow decrease in the rate of energy loss with increasing Z. The qualitative difference in stopping power behavior at high energies between a gas (He) and the other materials shown in Fig. 23.2 is due to the density effect correction, δ, discussed below. The stopping power functions are characterized by broad minima whose position drops from $\beta\gamma = 3.5$ to 3.0 as Z goes from 7 to 100.

In practical cases, most relativistic particles (*e.g.*, cosmic-ray muons) have energy loss rates close to the minimum, and are said to be minimum ionizing particles, or mip's.

Eq. (23.1) may be integrated to find the total range R for a particle which loses energy only through ionization. Since dE/dx depends only on β, R/M is a function of E/M or pc/M. In practice, range is a useful concept only for low-energy hadrons ($R \lesssim \lambda_I$, where λ_I is the nuclear interaction length), and for muons below a few hundred GeV (above which radiative effects dominate). R/M as a function of $\beta\gamma = pc/M$ is shown for a variety of materials in Fig. 23.3.

For a particle with mass M and momentum $M\beta\gamma c$, $T_{\rm max}$ is given by

$$T_{\rm max} = \frac{2m_e c^2 \, \beta^2 \gamma^2}{1 + 2\gamma m_e/M + (m_e/M)^2} \ . \tag{23.2}$$

It is usual [1,2] to make the "low-energy" approximation

$T_{\rm max} = 2m_e c^2 \, \beta^2\gamma^2$, valid for $2\gamma m_e/M \ll 1$; this, in fact, is done implicitly in many standard references. For pion in copper, the error thus introduced into dE/dx is greater than 6% at 100 GeV. The correct expression should be used.

At energies of order 100 GeV, the maximum 4-momentum transfer to the electron can exceed 1 GeV/c, where structure effects significantly modify the cross sections. This problem has been investigated by J.D. Jackson [6], who concluded that for hadrons (but not for large nuclei) corrections to dE/dx are negligible below energies where radiative

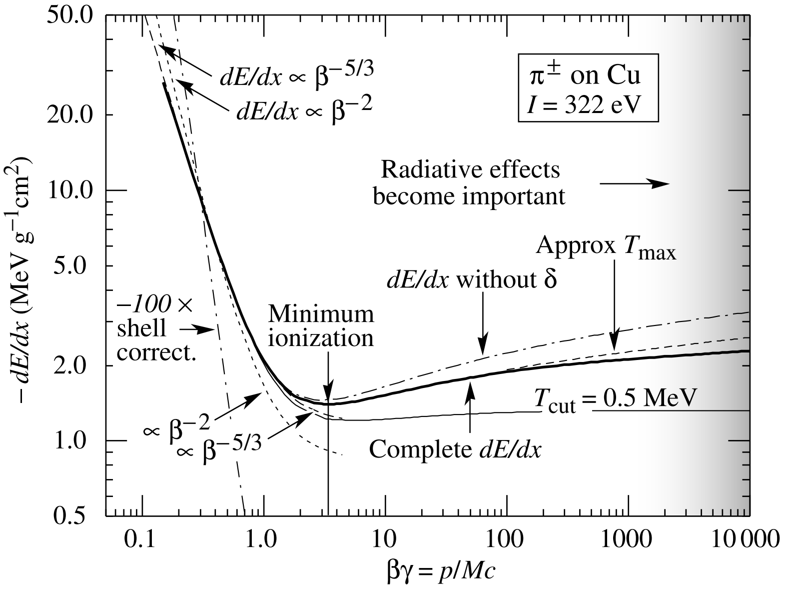

Figure 23.1: Energy loss rate in copper. The function without the density effect correction is also shown, as is the shell correction and two low-energy approximations.

effects dominate. While the cross section for rare hard collisions is modified, the average stopping power, dominated by many softer collisions, is almost unchanged.

The mean excitation energy I is $(10 \pm 1\ \text{eV}) \times Z$ for elements heavier than oxygen. The values adopted by the ICRU for the chemical elements [7] are now in wide use; these are shown in Fig. 23.4. Machine-readable versions can also be found [8]. Given the availability of these constants and their variation with atomic structure, there seems little point to depending upon approximate formulae, as was done in the past.

A shell correction is often included in the square brackets of Eq. (23.1) [3,5,7], to correct for atomic binding having been neglected in calculating some of the contributions to Eq. (23.1). We show the Barkas form [3] in Fig. 23.1. For copper it contributes about 1% at $\beta\gamma = 0.3$ (kinetic energy 6 MeV for a pion), and the correction decreases very rapidly with energy. While it is negligible for high-energy physics applications, this and other low-energy corrections must be taken into account at lower energies, such as those encountered in medical physics.

As the particle energy increases, its electric field flattens and extends, so that the distant-collision contribution to Eq. (23.1) increases as $\ln \beta\gamma$. However, real media become polarized, limiting the field extension and effectively truncating this part of the logarithmic rise [4,9–13]. At very high energies,

$$\delta/2 \rightarrow \ln(\hbar\omega_p/I) + \ln\beta\gamma - 1/2\ , \tag{23.3}$$

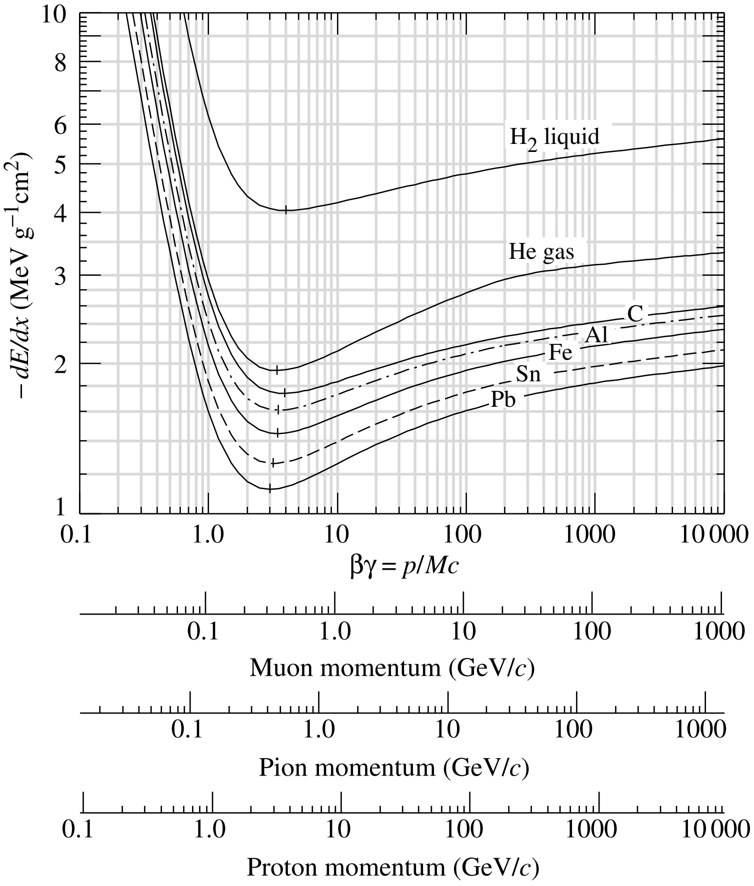

Figure 23.2: Energy loss rate in liquid (bubble chamber) hydrogen, gaseous helium, carbon, aluminum, tin, and lead.

where $\delta/2$ is the density effect correction introduced in Eq. (23.1) and $\hbar\omega_p$ is the plasma energy defined in Table 23.1. A comparison with Eq. (23.1) shows that $|dE/dx|$ then grows as $\ln \beta\gamma$ rather than $\ln \beta^2\gamma^2$, and that the mean excitation energy I is replaced by the plasma energy $\hbar\omega_p$. The stopping power as calculated with and without the density effect correction is shown in Fig. 23.1. Since the plasma frequency scales as the square root of the electron density, the correction is much larger for a liquid or solid than for a gas, as is illustrated by the examples in Fig. 23.2.

The remaining relativistic rise can be attributed to large energy transfers to a few electrons. If these escape or are otherwise accounted for separately, the energy deposited in an absorbing layer (in contrast to the energy lost by the particle) approaches a constant value, the Fermi plateau (see Sec. 23.3 below). The curve in Fig. 23.1 labeled "$T_{\rm cut} = 0.5$ MeV" illustrates this behavior. At extreme energies (*e.g.*, 400 GeV for muons

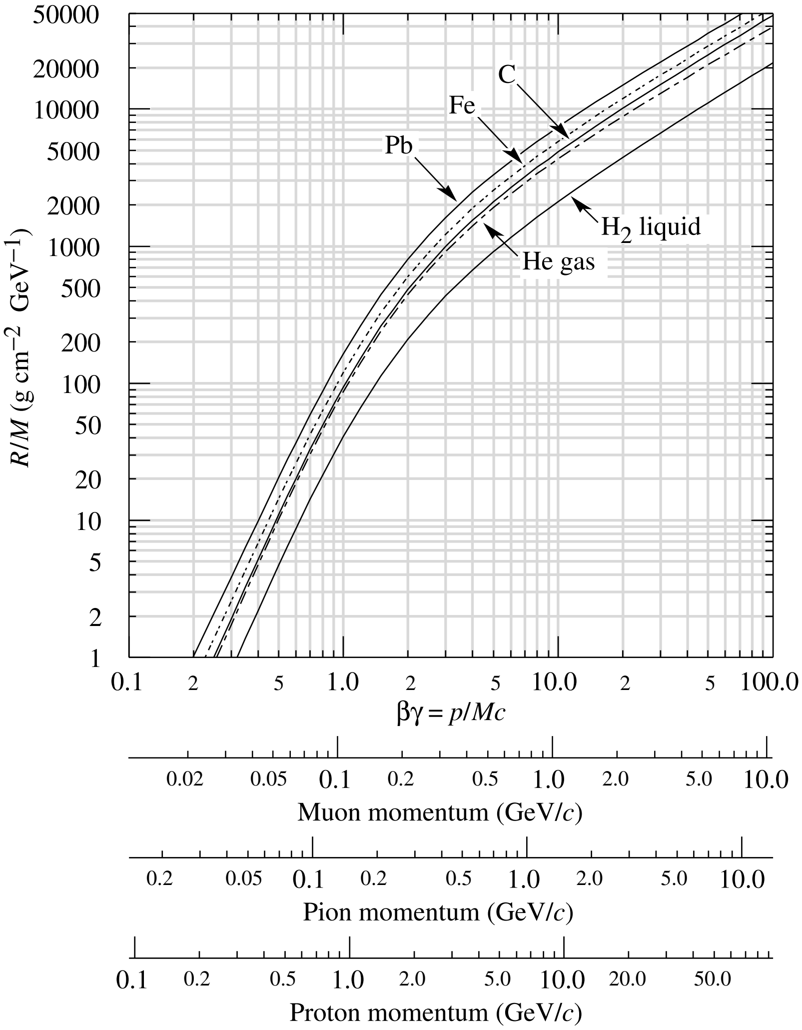

Figure 23.3: Range of heavy charged particles in liquid (bubble chamber) hydrogen, helium gas, carbon, iron, and lead. For example: For a K^+ whose momentum is 700 MeV/c, $\beta\gamma = 1.42$. For lead we read $R/M \approx 396$, and so the range is 195 g cm^{-2}.

or pions in iron), radiative effects become important. These are especially relevant for high-energy muons, as discussed in Sec. 23.9.

For particles moving more slowly than atomic electrons, the above discussion is inapplicable. At velocities $\alpha z \gtrsim \beta \gtrsim 10^{-3}$ or slightly lower, the total energy-loss rate is proportional to β, and non-ionizing nuclear recoil energy loss contributes substantially to the total [14]. For protons in silicon, $|dE/dx| = 61.2\,\beta$ GeV cm^2 g^{-1} for $\beta < 0.005$; the peak occurs at $\beta = 0.0126$, where $|dE/dx| = 522$ MeV cm^2 g^{-1}. In neutron-scattering

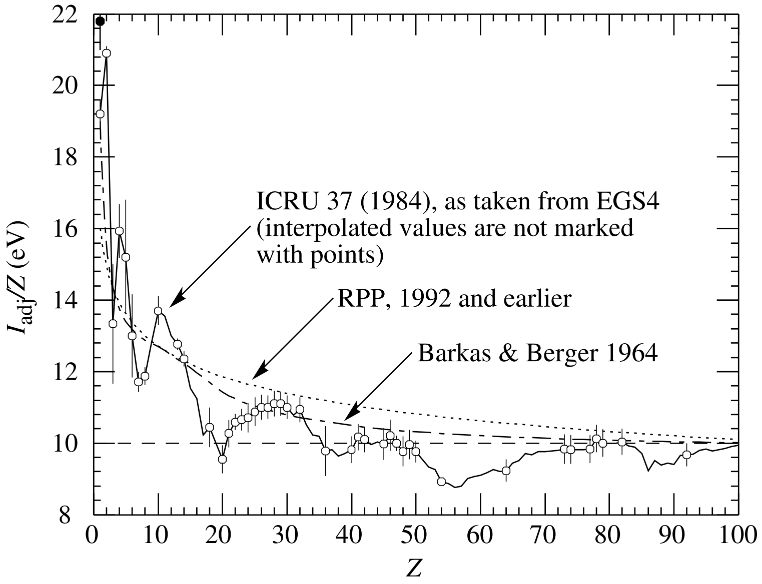

Figure 23.4: Excitation energies (divided by Z) as adopted by the ICRU [7]. Those based on measurement are shown by points with error flags; the interpolated values are simply joined. The solid point is for liquid H_2; the open point at 19.2 is for H_2 gas. Also shown are curves based on two approximate formulae.

experiments, light output in scintillator has been observed for recoil protons with energies as low as 30 eV [15].

It is often stated that for $\beta \gtrsim z/137$, $|dE/dx|$ falls as β^{-2} before reaching the broad minimum at $\beta\gamma \approx 3.0$–3.5. In fact, the slope is nowhere this great, and $|dE/dx| \propto \beta^{-5/3}$ provides a very good approximation to the actual function out to $\beta\gamma > 1$. This behavior is shown in Fig. 23.1, along with the traditional β^{-2} proportionality.

The quantity $(dE/dx)\delta x$ is the mean energy loss via interaction with electrons in a layer of the medium with thickness δx. For finite δx, there are fluctuations in the actual energy loss. The distribution is skewed toward high values (the Landau tail) [1,16]. Only for a thick layer $[(dE/dx)\delta x \gg T_{\rm max}]$ is the distribution nearly Gaussian. The large fluctuations in the energy loss are due to the small number of collisions involving large energy transfers. The fluctuations are smaller for the so-called restricted energy loss rate, as discussed in Sec. 23.3 below.

A mixture or compound can be thought of as made up of thin layers of pure elements in the right proportion (Bragg additivity). In this case,

$$\frac{dE}{dx} = \sum w_j \left. \frac{dE}{dx} \right|_j , \tag{23.4}$$

where $dE/dx|_j$ is the mean rate of energy loss (in MeV g cm^{-2}) in the jth element. Eq. (23.1) can be inserted into Eq. (23.4) to find expressions for $\langle Z/A \rangle$, $\langle I \rangle$, and $\langle \delta \rangle$; for example, $\langle Z/A \rangle = \sum w_j Z_j / A_j = \sum n_j Z_j / \sum n_j A_j$. However, $\langle I \rangle$ as defined this way is an underestimate, because in a compound electrons are more tightly bound than in the free elements, and $\langle \delta \rangle$ as calculated this way has little relevance, because it is the electron density which matters. If possible, one uses the tables given in Refs. 13 and 12, which include effective excitation energies and interpolation coefficients for calculating the density effect correction for the chemical elements and nearly 200 mixtures and compounds. If a compound or mixture is not found, then one uses the recipe for δ given in Ref. 10 (or Ref. 8), and calculates $\langle I \rangle$ according to the discussion in Ref. 11. (Note the "13%" rule!)

Ionization losses by electrons and positrons [12] are not discussed here. Above the critical energy, which is a few tens of MeV in most materials, bremsstrahlung is the dominant source of energy loss. This important case is discussed below. The contributions of various electron energy-loss processes in lead are shown in Fig. 24.4.

23.3. Restricted energy loss rates for relativistic ionizing particles

Fluctuations in energy loss are due mainly to the production of a few high-energy knock-on electrons. Practical detectors often measure the energy *deposited*, not the energy *lost*. When energy is carried off by energetic knock-on electrons, it is more appropriate to consider the mean energy loss excluding energy transfers greater than some cutoff $T_{\rm cut}$. The restricted energy loss rate is

$$-\left. \frac{dE}{dx} \right|_{T<T_{\rm cut}} = K z^2 \frac{Z}{A} \frac{1}{\beta^2} \left[\frac{1}{2} \ln \frac{2 m_e c^2 \beta^2 \gamma^2 T_{\rm upper}}{I^2} - \frac{\beta^2}{2} \left(1 + \frac{T_{\rm upper}}{T_{\rm max}} \right) - \frac{\delta}{2} \right] \tag{23.5}$$

where $T_{\rm upper} = {\rm MIN}(T_{\rm cut}, T_{\rm max})$. This form agrees with the equation given in previous editions of this *Review* [17] for $T_{\rm cut} \ll T_{\rm max}$ but smoothly joins the normal Bethe-Bloch function (Eq. (23.1)) for $T_{\rm cut} > T_{\rm max}$.